Physical Modeling of Hot-Carrier Degradation in nLDMOS Transistors

Y. Wimmer* S. Tyaginov*,†, F. Rudolf*, K. Rupp*, M. Bina*, H. Enichlmair°, J.-M. Park°,
R. Minixhofer°, H. Ceric*, and T. Grasser*
* Christian Doppler Laboratory for Reliability Issues in Microelectronics at the Institute for Microelectronics,
Vienna University of Technology, Gußhausstraße 27-29, A-1040 Vienna, Austria
*Institute for Microelectronics, Vienna University of Technology, Gußhausstraße 27-29, A-1040 Wien, Austria
†Ioffe Institute, 26 Polytekhnicheskaya, St Petersburg 194021, Russia
°ams AG, Tobelbader Strasse 30, A-8141 Unterpremstätten, Austria
Email: wimmer@iue.tuwien.ac.at

***Abstract*—Our physics-based HCD model has been validated using scaled CMOS transistors in our previous work. In this work we apply this model for the first time to a high-voltage nLDMOS device. For the calculation of the degrading behaviour the Boltzmann transport equation solver ViennaSHE is used which also requires high quality adaptive meshing. We discuss the influence of the different model components in the different device regions. Finally we compare the model to experimental degradation results and show that each one gives a significant contribution to the result and that all of them are needed in order to satisfactorily fit the experimental data.**

I. Introduction

The LDMOS transistor is one of the most popular devices employed in mixed-signal integrated circuits and in high-voltage automotive applications [1]. Hot-carrier degradation (HCD) still remains one of the main reliability concerns in these devices [1], [2], [3], [4]. This makes a predictive physical model for HCD in LDMOS very attractive. At the same time, such a model is extremely challenging to develop because of the complexity of the HCD-phenomenon and the complicated topological structure of the LDMOS.

In fact, the physical origin of HCD is related to the generation of traps at or near the Si/SiO_2 interface. This generation is due to hot and cold carriers triggering single-carrier and multiple-carrier dissociation mechanisms [5], [6], [7]. Thus, the key information needed for proper HCD modeling is the carrier energy distribution functions (DFs), which determine the rates of both aforementioned processes. This information can be obtained from a solution of the Boltzmann transport equation (BTE) [5]. Such a solution is challenging even for planar CMOS devices with a simpler architecture and becomes extremely demanding for such devices as the LDMOS transistor. This device has a non-planar interface with a non-trivial distribution of the electric field near the bird's beak (see Figs. 1,3), where the impact ionization spot, and hence the hot-carrier degradation spot are located [3], [4].

In this work we apply our physics-based HCD model – which has been validated using scaled CMOS transistors with a gate length as short as 65 nm [6], [7] – to represent the linear drain current change due to HCD in a high-voltage device, i.e. the nLDMOS, for the first time.

II. Experiment

Experiments were carried out on nLDMOS devices fabricated on a standard 0.35 μm process with the maximum operating drain voltage V_{ds} of 20 V. The devices were subjected to hot-carrier stress at a fixed gate voltage of V_{gs} = 2 V and three different drain voltages: V_{ds} = 18, 20, and 22 V at a temperature of 300 K. To assess HCD, the change in the linear drain current ΔI_{dlin} (measured at V_{ds} = 0.1 V and V_{gs} = 2.4 V) was recorded as a function of stress time, see Fig. 6).

III. Simulation Framework

Our HCD model consists of three main components: carrier transport treatment, description of the defect generation kinetics, and modeling of the degraded devices [6], [7], see Fig. 2. Device geometry and doping profiles were obtained by Synopsis Sentaurus Process simulator [8]. The device characteristics of the fresh transistor were then calculated using the MINIMOS-NT drift-diffusion simulator. $I_{\mathrm{ds}} - V_{\mathrm{gs}}$ curves at V_{ds} = 0.1 V and V_{ds} = 20.1 V as well as $I_{\mathrm{ds}} - V_{\mathrm{ds}}$ curves at V_{gs} = 0.66 V, 1.32 V, 1.98 V , 2.64 V and 3.30 V could be reproduced with reasonable accuracy.

In order to determine DFs we continued using the free open source deterministic Boltzmann transport equation solver ViennaSHE, developed at our Institute [5], [6], [7], [9]. For simulating such a large device with ViennaSHE, highly adaptive meshing is needed, keeping the number of cells (and therefore the number of variables) in a moderate range, but still providing a fine enough mesh in the important regions, i.e. in the channel, at the bird's beak and in regions with high doping gradients. Furthermore, the meshing framework has to be capable to properly handle curved material interfaces, an issue that is often not properly addressed in meshing tools using quadtree-based mesh generation [10]. For re-meshing the device in this work we used the free open source ViennaMesh [11] framework, which meets these requirements perfectly [12]. The adaptive mesh was generated using the distance from the gate contact and the gradient of the built-in potential (see Fig. 3) as refinement criteria. It contains ∼11 000 points and is very fine near the interface and in other important regions, but much coarser in the Si bulk.

978-1-4799-7274-6/14/$31.00 ©2014 IEEE

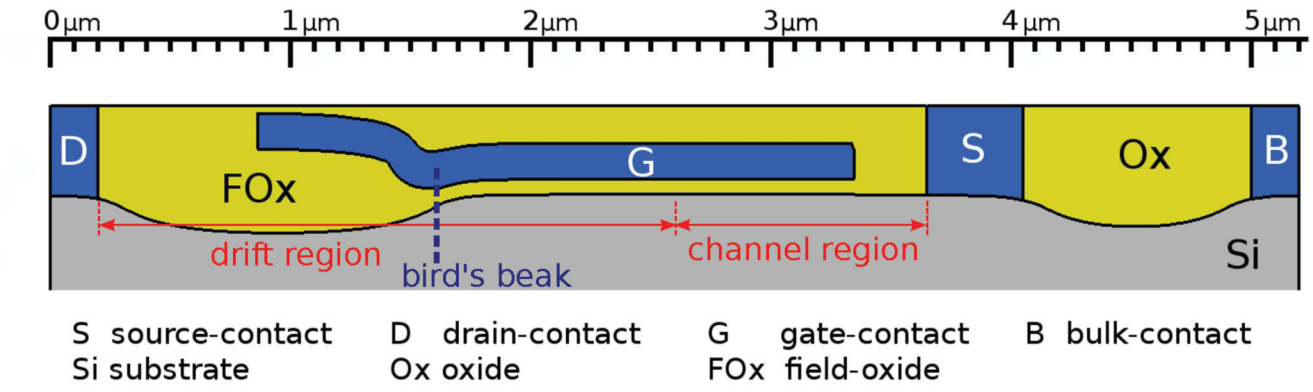

Fig. 1. Schematic representation of the near-interface section of the nLDMOS with all the characteristic sections labeled.

We repeated MINIMOS-NT simulations to be sure that the simulation results do not change appreciably when we refine the grid.

Using these drift-diffusion solutions as an initial guess for ViennaSHE, we were able to simulate a series of carrier DFs for the given stress conditions at each point of the Si/SiO_2 interface. The spherical-harmonics-expansion method used in this solver guarantees smooth DF-curves down to very small values where a Monte-Carlo-method would already show large noise [13], a huge advantage since the DFs spread over over dozens of orders of magnitude (see Fig. 5 a).

The bond-breakage rates are then calculated using our physics based HCD model. In this model the Si-H bonds are treated as truncated harmonic oscillators (see Fig. 4) which are bombarded by electrons and holes of different energy. The energy-distribution of those carriers is defined by the DFs. There are two main competing pathways of the Si-H bond dissociation reaction [6], [7], [14]. The first one can occur if a solitary high-energetic carrier hits the bond. In this case one of the bonding electrons is excited to an antibonding (AB) state, a process called the AB-process. The second pathway is related to the multivibrational excitation (MVE) of the bond by a series of carriers with energies below the threshold for triggering the AB-mechanism. This is referred to as the MVE-process. These competing mechanisms as well as all their possible superpositions (see Fig. Fig. 4) are considered self-consistently within a set of rate equations [6], [7].

Two other factors which impact the defect generation rates are, first, the reduction of the activation energy (the energy to break a bond from its ground state) E_a due to the interaction of the oxide electric field F with the dipole moment of the bond d and, second, statistical fluctuations of this energy caused by the structural disorder at the interface between crystalline Si and amorphous SiO_2. The first effect is modeled by the product $d \times F$ with $d = 5.6 \times 10^2 \mathrm{Cm}$ [15]. For the second effect we assume that E_a obeys a normal distribution with the mean value of $\langle E_a \rangle = 1.6\,\mathrm{eV}$ and $\sigma_E = 0.13\,\mathrm{eV}$, close to the values used previously for scaled devices (1.5 and 0.15 eV, respectively) [6], [7]. However, the parameters $\langle E_a \rangle$ and σ_E are weakly technology depended.

IV. Results and Discussion

Two families of carrier DFs at the drain area ($x = 0.2\,\mu$m) and in the vicinity of the bird's beak ($x = 1.2\,\mu$m, cf. Fig. 1) simulated for $V_{ds} = 18$, 20 and 22 V are plotted in Fig. 5 a. All of them are severely distorted from equilibrium. DFs near the drain show a Maxwellian-like decay at low energies. The interface state density ($N_{it}(x)$) profiles computed for two stress times of 10 s and 1 Ms for $V_{gs} = 2\,\mathrm{V}$ and $V_{ds} = 20\,\mathrm{V}$ are shown in Fig. 5 b.

In order to understand the different contributions to the model, it is instructive to compare the $N_{it}(x)$ profile with others, evaluated each disregarding exactly one component of the model (Fig. 5 c-f). It can be seen that carriers near the drain are rather hot, thereby leading to a drain N_{it} peak, cf. [16]. If one of the AB- or MVE-mechanisms is deactivated, this peak does not disappear, therefore we conclude that both processes are saturated. Another peak is visible in the vicinity of the bird's beak which is consistent with previous findings [3], [4]. This peak is clearly visible in all figures but Fig. 5 c. Since it disappears if the AB-process rate is neglected we conclude that this is the dominant mechanism causing it.
The MVE-mechanism, can be held responsible for the channel N_{it} maximum pronounced at $x \sim 2.8\,\mu$m. If this MVE-mechanisms is ignored (Fig. 5 d), the $N_{it}(x)$ profile follows the changes of $F(x)$ via the $d \times F$ interaction but the peak disappears. This can be easily understood because since carriers are rather cold near the source, there are nearly no carriers with high enough energies to excite the bond from its ground state in an AB-process. The situation is exactly flipped at the drain and in the bird's beak vicinity, where there is a high concentration of hot carriers that do not need a pre-heated bond (by the MVE-processes) for creating a defect.
Furthermore, one can see that if $d \times F$ is neglected (Fig. 5 e), a ledge in $N_{it}(x)$ appears for the lateral coordinate x between 1.5μm and 2.5μm. This result agrees well with our previous results [6], [17] obtained for 5V n-MOSFETS with the gate length of 0.5μm subjected to hot-carrier stress at $V_{ds} \geq 6.25$V. These findings are also in good agreement with the results

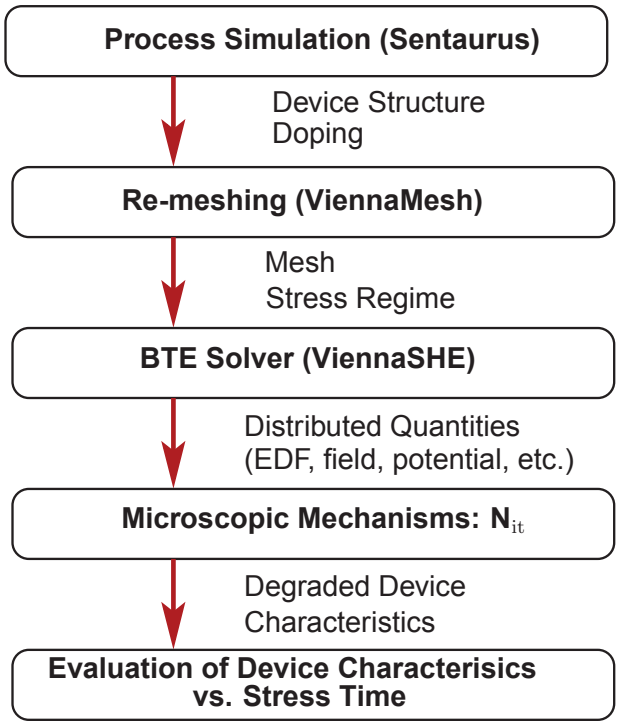

Fig. 2. Flowchart of the simulation framework. The geometry was modeled using Sentaurus Process simulator and meshed using the ViennaMesh tool. Then the electrostatics of the fresh device were calculated using MINIMOS NT. Next ViennaSHE was used to describe the DFs needed to calculate the defect generation kinetics, followed by modeling of the degraded device.

published by Bravaix et al. [18].
The activation energy dispersion shifts the N_{it} profiles towards higher values (Fig. 5 f). This becomes clear considering that the E_{a} fluctuations offer lower activation energies while additionally the DFs are higher at lower energies. As an interplay of these effects more bonds can be excited as if E_{a} was fixed to a certain value.

Fig. 6 shows good agreement between experimental and simulated $\Delta I_{\mathrm{dlin}}(t)$ data. Here we also see the contributions of the different model components are visible again in the curves calculated neglecting one model component.
The AB-process, for example, becomes important for longer stress times under all stress conditions. This is because HCD at short times is controlled by the drain and channel N_{it} maxima which are related to the MVE-mechanism. Therefore it is not surprising that if the MVE-mechanism is ignored, ΔI_{dlin} is severely underestimated at short stress times.
One can also see that the effect of the activation energy reduction ($d \times F$) becomes less pronounced for long stress times and at higher V_{ds}. Finally, the statistical variations in E_{a} substantially enhance HCD although their impact is less pronounced at higher stress voltages. This tendency appears reasonable because if carriers are already hot enough, further reduction of the activation energy would not yield additional degradation.

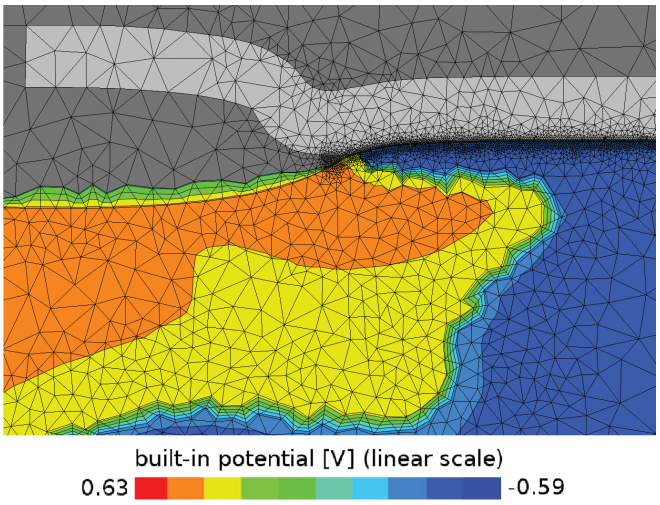

Fig. 3. Detail of the adaptive mesh which is used for calculating the carrier energy distribution functions using ViennaSHE. The mesh is fine near the Si/SiO_2 interface but coarse in the Si bulk. The criteria for mesh refinement were the distance from the gate contact and the built-in potential represented by the color map above.

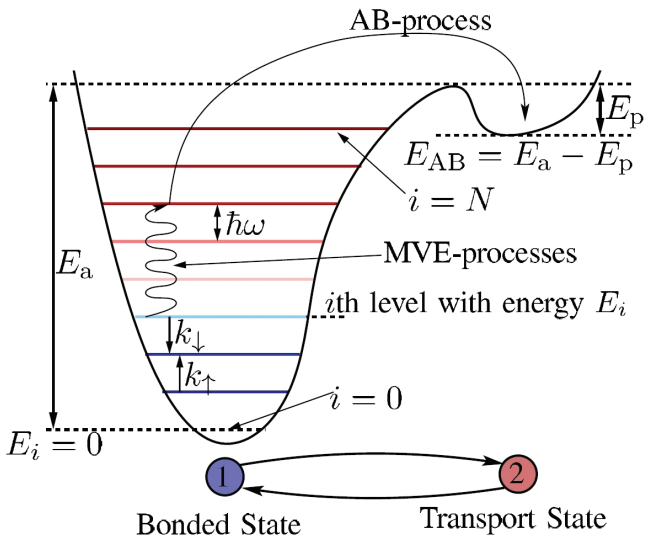

Fig. 4. Truncated harmonic oscillator model of the Si-H bond used for the derivation of our HCD model. The bond is broken when the transport state 2 is reached. The energy necessary for this process can be lowered by precedent MVE-processes exciting the bond into a higher energy level of the harmonic oscillator. The activation Energy E_{a}, henceforth the depth of the harmonic oscillator potential, is Gaussian distributed with the mean value of $\langle E_{\mathrm{a}} \rangle$ = 1.6 eV and σ_{E} = 0.13 eV. Furthermore the value of E_{a} is also modeled to vary due to interaction with the electric field.

V. Conclusions

We have successfully applied our physical model of hot-carrier degradation, which is based on thorough carrier transport treatment, to the nLDMOS transistor. The model is capable of representing the linear drain current change during hot-carrier stress under different values of V_{ds} and stress times. We have also analyzed the importance of several model components such as the competing mechanisms of bond dissociation, stochastic variations of the activation energy, and

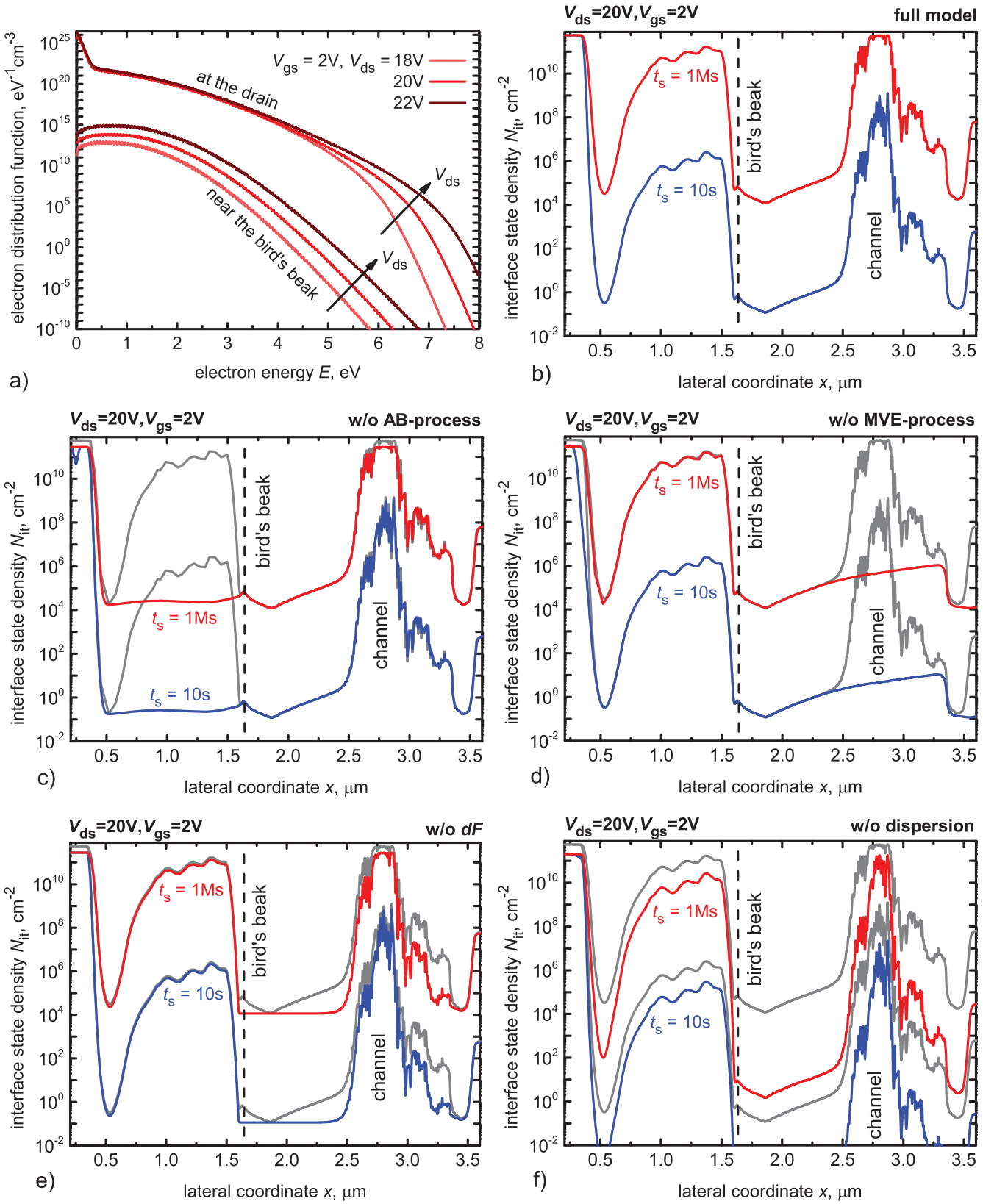

Fig. 5. a) Non-equilibrium electron DFs simulated for $V_{\rm ds}$ = 18, 20 and 22 V at the position near the drain and at the bird's beak. b)-f) $N_{\rm it}(x)$ profiles after stress time of 10 s and 1 Ms for $V_{\rm gs}$ = 2 V and $V_{\rm ds}$ = 20 V. For comparison, also $N_{\rm it}(x)$ profiles each computed ignoring only one of the model components c)-f) are depicted, here the grey curves shows the result of the full model.

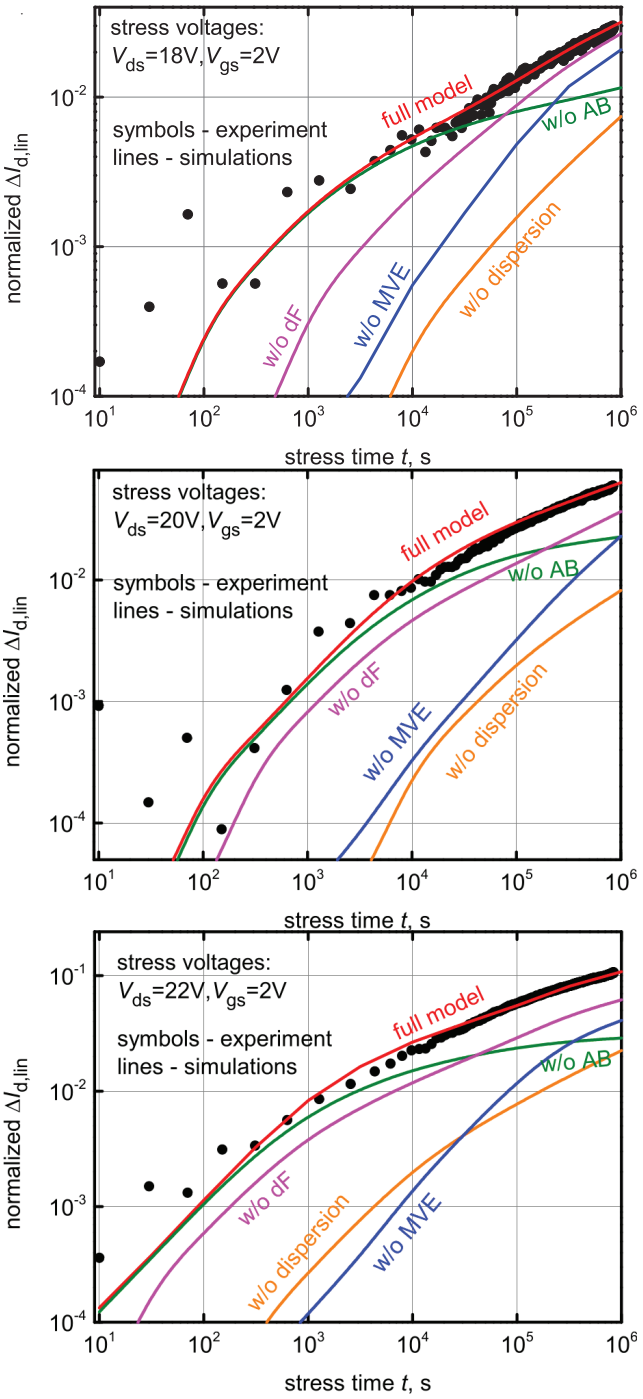

Fig. 6. Normalized linear drain current change: experiment vs. simulations, obtained for a fixed V_{gs} = 2.0 V and a series of three different V_{ds} = 18, 20, and 22 V. To analyze the importance of different model components (AB- and MVE-mechanisms, the activation energy reduction due to the field-dipole interaction, and statistical variations of this energy), $\Delta I_{\mathrm{dlin}}(t)$ curves were also calculated each neglecting only one of these components. It is clearly visible that all model components are needed to correctly describe the experimental data.

its reduction due to the field-dipole interactions. We conclude that different model components become dominant in different device regions. Finally we have demonstrated that all of them contribute and are needed for a satisfactorily representing the experimental degradation data.

Acknowledgment

The authors acknowledge support by the Austrian Science Fund (FWF), grant P23598, by the European Union FP7 project ATHENIS_3D (grant No 619246) and by the European Research Council (ERC) project MOSILSPIN (grant No 247056).

References

[1] S. Reggiani, G. Barone, E. Gnani, A. Gnudi, G. Baccarani, S. Poli, R. Wise, M.-Y. Chuang, W. Tian, S. Pendharkar, and M. Denison, "Characterization and Modeling of Electrical Stress Degradation in STI-based Integrated Power Devices," *Solid-State Electronics*, vol. in press, 2014.

[2] A. Ludikhuize, M. Slotboom, A. Nezar, N. Nowlin, and R. Brock, "Analysis of hot-carrier-induced degradation and snapback in submicron 50v lateral mos transistors," in *Proc. International Symposium on Power Semiconductor devices and ICs*, 1997, pp. 53–56.

[3] P. Moens, G. van den Bosch, and G. Groeseneken, "Competing hot carrier degradation mechanisms in lateral n-type dmos transistors," in *Proc. International Reliability Physics Symposium (IRPS)*, 2003, pp. 214–221.

[4] D. Brisbin, P. Lindorfer, and P. Chaparala, "Substrate current independent hot carrier degradation in nldmos devices," in *Proc. International Reliability Physics Symposium (IRPS)*, 2006, pp. 329–333.

[5] M. Bina, K. Rupp, S. Tyaginov, O. Triebl, and T. Grasser, "Modeling of Hot Carrier Degradation Using a Spherical Harmonics Expansion of the Bipolar Boltzmann Transport Equation," in *Proc. International Electron Devices Meeting (IEDM)*, 2012, pp. 713–716.

[6] S. Tyaginov, M. Bina, J. Franco, D. Osintsev, O. Triebl, B. Kaczer, and T. Grasser, "Physical modeling of hot-carrier degradation for short- and long-channel mosfets," in *Proc. International Reliability Physics Symposium (IRPS)*, 2014, pp. XT.16–1–16–8.

[7] M. Bina, S. Tyaginov, J. Franco, Y. Wimmer, D. Osinstev, B. Kaczer, T. Grasser *et al.*, "Predictive Hot-Carrier Modeling of n-channel MOSFETs," *IEEE Transactions on Electron Devices*, vol. in press, 2014.

[8] *Synopsis, Sentaurus Process, Advanced Simulator for Process Technologies*.

[9] http://viennashe.sourceforge.net/, 2014.

[10] S.-W. Cheng, T. K. Dey, and J. R. Shewchuk, *Delaunay Mesh Generation*. CRC Press, 2013.

[11] http://viennamesh.sourceforge.net/, 2014.

[12] F. Rudolf, J. Weinbub, K. Rupp, and S. Selberherr, "The Meshing Framework ViennaMesh for Finite Element Applications," *Journal of Computational and Applied Mathematics*, vol. 167, pp. 166–177, 2014.

[13] S.-M. Hong, A. Pham, and C. Jungemann, *Deterministic Solvers for the Boltzmann Transport Equation*, springer ed., 2011.

[14] W. McMahon, K. Matsuda, J. Lee, K. Hess, and J. Lyding, "The Effects of a Multiple Carrier Model of Interface States Generation of Lifetime Extraction for MOSFETs," in *Proc. Int. Conf. Mod. Sim. Micro*, vol. 1, 2002, pp. 576–579.

[15] C. Guerin, V. Huard, and A. Bravaix, "General Framework about Defect Creation at the Si/SiO_2 Interface," *Journ. Appl. Phys.*, vol. 105, pp. 114 513–1–114 513–12, 2009.

[16] M. Antoniou, F. Udrea, E. K. C. Tee, Y. Hao, S. Pilkington, K. K. Yaw, D. Pal, and A. H. and, "Interface Charge Trapping and Hot Carrier Reliability in High Voltage SOI SJ LDMOSFET," in *Proc. International Symposium on Power Semiconductor devices and ICs*, 2011, pp. 336–339.

[17] S. Tyaginov, I. Starkov, O. Triebl, J. Cervenka, C. Jungemann, S. Carniello, J. Park, H. Enichlmail, C. Kernstock, E. Seebacher, R. Minixhofer, H. Ceric, and T. Grasser, "Interface Traps Density-of-states as a Vital Component for Hot-carrier Degradation Modeling," *Microelectronics Reliability*, vol. 50, pp. 1267–1272, 2010.

[18] Y. Randriamihaja, A. Zaka, V. Huard, M. Rafik, D. Rideau, D. Roy, A. Bravaix, and P. Palestri, "Hot Carrier Degradation: From Defect Creation Modeling to Their Impact on NMOS Parameters," in *Proc. International Reliability Physics Symposium (IRPS)*, 2012, pp. 1–4.